Routing Based on Dynamic Reliability in Massive LEO Satellite Optical Networks

Yating Wei
Zhengzhou University
Zhengzhou, China
weiyating@gs.zzu.edu.cn

Ruijie Zhu
Zhengzhou University
Zhengzhou, China
zhuruijie@zzu.edu.cn

Yudong Zhang
Zhengzhou University
Zhengzhou, China
zhang_zyd@163.com

Chao Xi
Space Star Technology CO., LTD
Beijing, China
xichaofh@163.com

Wenchao Zhang
Zhengzhou University
Zhengzhou, China
zhangwenchao9066@163.com

Yajun Li
Zhengzhou University
Zhengzhou, China
liyajun@gs.zzu.edu.cn

Xueyuan Qiao
Space Star Technology CO., LTD
Beijing, China
xiaoqiaofly@163.com

Bo Yang
Space Star Technology CO., LTD
Beijing, China
bagoiyb@126.com

***Abstract*—We propose a routing based on dynamic reliability (RDR) algorithm considering space risks in massive LEO satellite optical networks. Simulation results show that it can achieve a lower transmission failure rate than three state-of-art algorithms.**

Keywords—Satellite reliable routing, massive LEO satellite optical network, space risk prediction

I. INTRODUCTION

In recent years, with the rapid development of massive low earth orbit (LEO) satellite optical networks(LSONs), both the scale of constellations and the complexity of near-earth space are greatly increasing [1]. According to the data released by NASA Johnson Space Center, as of December 2022, there are 9803 trackable spacecrafts and 16054 trackable debris in near-earth space [2]. Therefore, a tremendous amount of space risks including collisions, failures, and optical link blockages increased significantly, which weakens optical inter-satellite links (OISLs) reliability in the routing process. As the representative of large-scale LEO constellations, Starlink is planned to contain more than 43000 satellites, and thus efficient and highly accurate space risk predictions are required [3]. Previous studies about service quality, load balancing, resource allocation and traffic allocation have been investigated [4-10]. However, they have not considered the impact of space debris, satellite failures, and sun outage on satellite optical networks. Meanwhile, most satellite collision studies optimize the Clohessy-Wiltshire equation and construct the artificial potential field method [11, 12]. However, these existing methods do not consider the calculation of risks of multiple elements. To meet the different reliability requirements of services of massive LEO satellite optical networks, satellite collisions, failures, and sun outage should be considered in the routing process.

In this paper, we proposed a routing based on dynamic reliability (RDR) algorithm to solve the problem of the vulnerability of satellites and OISLs in LSONs. Firstly, we proposed the pipeline model to reduce the calculation and the computational complexity by determining high-risk areas in advance according to orbit parameters. Then, we optimized the risk probability prediction model. Simulation results show good performance in terms of transmission failure rate (TFR).

This work was supported in part by the National Natural Science Foundation of China under Grant 62001422, 62036010, and Henan Scientific and Technology Innovation Talents No. 22HASTIT016.

II. SYSTEM MODEL

A. Pipeline risk prediction model

To improve the accuracy of LSON risk prediction, a pipeline risk assessment model with variable time granularity is proposed for the annular characteristics of satellite orbits shown in Fig. 1. The pipeline model is used to package the orbit range of the satellite and control the spatial range of risk assessment.

The center lines of pipelines are the satellite orbits, which are calculated using the latest two line elements (TLE) data. The radius of a pipeline cross-section is determined by satellite safety distance and satellite wing deployment length. According to the regional spatial density, we define the time granularity TG for improving the precision and efficiency of risk prediction. The volume of risk prediction area for pipelines is calculated by:

$$V = \pi r^2 \int_{t_s}^{t_s+TG} v(t)\, dt \tag{1}$$

where r represents the radius of a pipeline cross-section, t_s is the prediction start time, TG indicates the time granularity, $v(t)$ denotes the satellite velocity function.

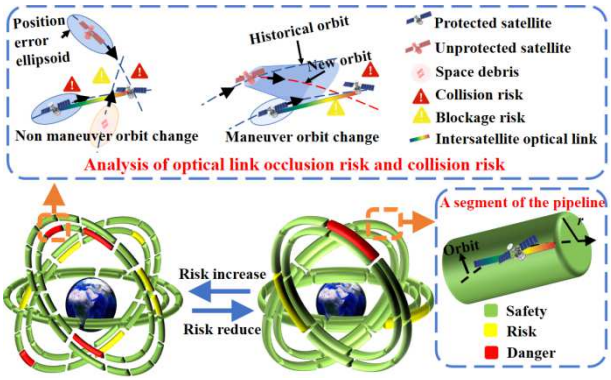

Fig. 1. Pipeline risk prediction model with variable time granularity

B. Satellite optical network model

In the satellite optical network routing process, the underlying satellite optical network is modeled as an undirected network graph $G_S(N_S, L_S)$, where N_S is the set of satellite nodes and L_S denotes the set of inter-satellite links. The selection of each hop depends on the satellite reliability R^S, time delay T^L, satellite node CPU resource C^S and laser link bandwidth resource B^L. Satellite reliability R^S consists of the reliability of satellite nodes R_N^S and inter-

satellite links R_L^S. Satellite node reliability contains satellite collision probability P_L^F and satellite failure probability P_N^F. The causes of satellite failure cover low battery, faults of major components, and space complex electromagnetic interference. The link reliability is decided by the failure probability of the optical transmitter in a certain direction of the satellite. According to historical data, both failure probability distribution follows the normal distribution.

III. ROUTING BASED ON DYNAMIC RELIABILITY ALGORITHM

We apply satellite reliability to develop a high-reliability routing strategy, which applies to scenarios that require high security and a low retransmission rate. To select a more reliable satellite node in the routing process, we comprehensively consider the collision probability and the satellite failure probability that affects the normal operation of the satellite. The model architecture of the RDR algorithm is shown in Fig. 2.

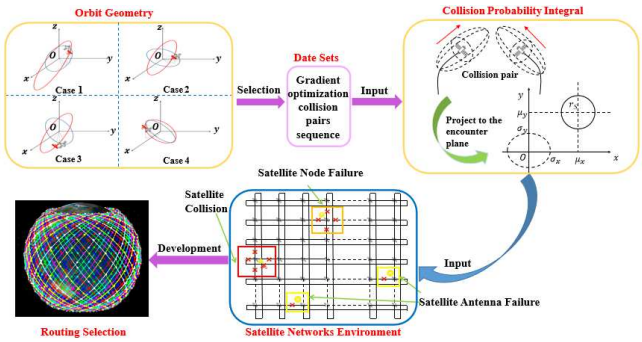

Fig. 2. The model architecture of the RDR algorithm

When there are no malicious approaches to maneuver orbit changes and intersections with other satellite tracks, the satellite operates normally and stably. We obtain the orbital inclination angle and the right ascension of the ascending node (RAAN) of the two satellites from TLE data. Taking advantage of the geometric relationship between them, the position of the intersection where a collision may occur can be achieved. Ω and φ are used to determine the spatial location of the intersection. They are deduced by:

$$\Omega = tan^{-1}\frac{(sin\,\Omega_2\ tan\,i_2 - sin\,\Omega_1\,tan\,i_1)}{(cos\,\Omega_2\,tan\,i_2 - cos\,\Omega_1\,tan\,i_1)} \tag{2}$$

$$\varphi = tan^{-1}(sin(\Omega - \Omega_1)\ tan\,i_1) \tag{3}$$

where i_1 and i_2 represent satellite inclinations, Ω_1 and Ω_2 indicate satellite RAAN.

To ensure the highest overall safety of the constellation, the sequence of collision pairs based on geometric selection is adjusted by gradient optimization processing. Each attribute has the same proportion in the initial stage. According to the principle of longest reserved avoidance collision time, we change the proportion of each attribute in the direction of the gradient.

Numerous previous studies about satellite collision probability revealed that the calculation of probability can be eventually transformed into calculating for an integral of the two-dimensional isotropic probability density function on the cross-section area of the encounter plane. To improve the risk calculating efficiency, the integration regions are optimized from ellipses to circles with the satellite safety distance as their radiuses. The satellite collision probability can be expressed by:

$$P^c = \iint_{(x-\mu_x)^2+(y-\mu_y)^2 \le r_S^2} \frac{1}{2\pi\sigma_x\sigma_y} exp\left[-\frac{1}{2}\left(\frac{x^2}{\sigma_x^2}+\frac{y^2}{\sigma_y^2}\right)\right] dx\,dy \tag{4}$$

where r_S represents the satellite safety distance, μ_x is the mean value of x under the encounter plane, μ_y denotes the mean value of y, σ_x indicates the variance of x, σ_y means the variance of y, and they all are under the encounter plane.

According to historical data and current studies, the failure probability of satellite nodes and links corresponds to normal distribution. Besides, each satellite failure can cause 4 optical links to be disconnected. Each satellite optical transmitter failure can cause one optical link to be disconnected. $P_N^F(P_{N_1}^F, P_{N_2}^F, \dots, P_{N_n}^F)$ denotes the failure probability of n satellite nodes. The failure probability of n inter-satellite links can be expressed by a set $P_L^F(P_{L_1}^F, P_{L_2}^F, \dots, P_{L_n}^F)$. $\sum_1^n(P_{N_i}^F + P_{L_i}^F)$ denotes the sum of the failure probability of each optical link. The expectation is μ_f, and the variance is σ_f.

In the process of selecting the next hop of the route, the nodes with high reliability are given priority. If the reliability of the two nodes is equal, the node with a lower delay will be selected. The satellite reliability probability is computed by:

$$R^S = \alpha \times (1 - P_N^F) + \beta \times (1 - P_L^F) + \gamma \times (1 - P^C) \tag{5}$$

where α, β, and γ are adjustment factors. P_N^F denotes satellite link failure probability, P_L^F expresses satellite link failure probability, and P^C indicates satellite collision probability.

IV. SIMULATION RESULT

Simulations are developed over two satellite optical networks, which are constructed based on the data published by the first phase of the Starlink constellation [3]. As the representative of the massive LSONs, each satellite in Starlink can establish optical communication links with two adjacent satellites in the same orbital plane and two other satellites in the adjacent orbital planes. Table I shows the parameters of the two constellations.

The reliability of each satellite is set to 100, the CPU resource of each satellite node is set to 10 and the bandwidth resource of each laser link is set to 50. The request generations follow the Poisson distribution. The comparison algorithms adopt the Dijkstra routing algorithm, the collision probability-based dynamic routing (CPDR) algorithm, and the failure probability-based dynamic routing (FPDR) algorithm. The evaluation metric is TFR, which refers to the rate of the number of failed service transmissions to the total number of service transmissions.

The performance of our algorithm is evaluated under different traffic loads. From Fig. 3, it can be found that the TFR decreases by 8.8% more than the Dijkstra routing algorithm in the 72×22 satellite optical network when the traffic load is 50 Erlang. Simultaneously, Fig. 4 shows that TFR can be decreased obviously when the satellite topology becomes large.

TABLE I. SIMULATION PARAMETERS

Parameters	***Values***	
Satellite optical network name	72×22 satellite optical network	72×22 satellite optical network
Total number of satellites	1584	396
Number of orbits	72	36
Number of satellites per plane	22	11
Satellite altitude	550km	550km
Inclination of orbit	53	53

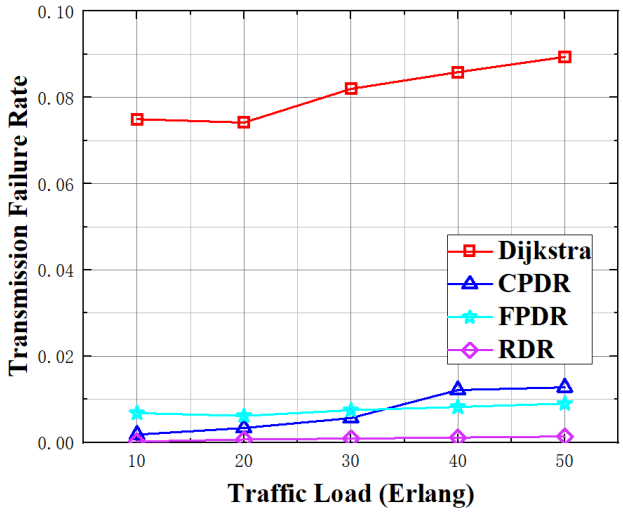

Fig. 3. TFR under different algorithms in the 72×22 satellite optical network

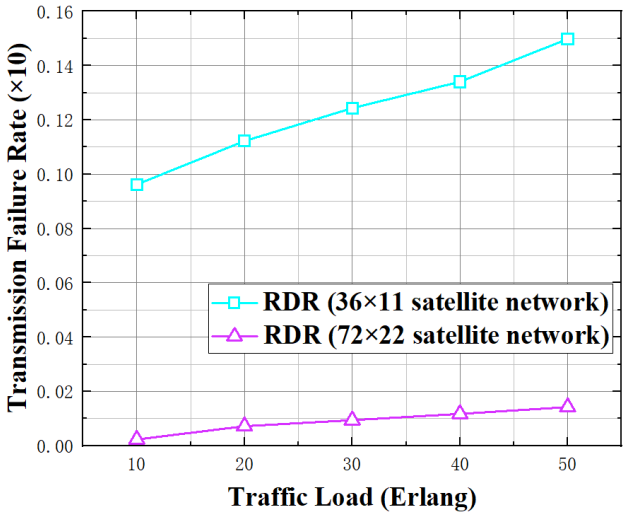

Fig. 4. TFR in different networks

V.CONCLUSION

We propose a collision probability method based on geometric screening, which concludes space filters and collision pair sequence optimization. Then, we develop a routing based on dynamic reliability (RDR) algorithm. Simulation results show that the RDR algorithm performs better than the state-of-art algorithms in TFR.

REFERENCES

[1] R. Zhu, G. Li, Y. Zhang, et al., "Load-Balanced Virtual Network Embedding Based on Deep Reinforcement Learning for 6G Regional Satellite Networks," *IEEE Transactions on Vehicular Technology*, 2023.

[2] "Space Missions and Satellite Box Score," Orbital Debris Quarterly News, 2022.

[3] T. Duan, et al., "Starlink Space Network-Enhanced Cyber–Physical Power System," IEEE T SMART GRID, 12.4, 3673-3675, 2021.

[4] P. Kumar, et al., "fybrrLink: Efficient QoS-Aware Routing in SDN Enabled Future Satellite Networks," TNSM, 19.3, 2107-2118, 2022.

[5] X. Deng, et al., "Distance-Based Back-Pressure Routing for Load-Balancing LEO Satellite Networks," TVT, 2022.

[6] H. Yang, et al., "Maximum Flow Routing Strategy for Space Information Network With Service Function Constraints," TWC, 21.5, 2909-2923, 2022.

[7] R. Zhu, P. Wang, et al., "Double-Agent Reinforced vNFC Deployment in EONs for Cloud-Edge Computing," *IEEE Journal of Lightwave Technology*, 2023.

[8] R. Zhu, G. Li, P. Wang, M. Xu, and S. Yu, "DRL Based Deadline-Driven Advance Reservation Allocation in EONs for Cloud-Edge Computing," *IEEE Internet of Things Journal*, vol.9, no.21, 2022.

[9] R. Zhu, S. Li, et al., "Energy-efficient Deep Reinforced Traffic Grooming in Elastic Optical Networks for Cloud-Fog Computing," *IEEE Internet of Things Journal*, vol.8, no.15, 2021.

[10] R. Zhu, A. Samuel, et al., "Protected Resource Allocation in Space Division Multiplexing-Elastic Optical Networks (SDM-EONs) with Fluctuating traffic," *Journal of Network and Computer Applications*, vol. 174, 2021.

[11] Z. Chen, et al., "Near-Earth Orbit Satellite Collision Probability Estimation and Collision Avoidance," CAC, 855-860, 2019.

[12] A. R. Hamed, et al., "Optimized Curvilinear Potential Field Based Multi-objective Satellite Collision Avoidance Maneuver," AC, 1-9, 2022.